DOI: 10.1002/ ((please add manuscript number))
Article type: Full Paper

Title
Tough and Self-Recoverable Thin Hydrogel Membranes for Biological Applications

Ya Nan Ye[1], Martin Frauenlob[1], Lei Wang[2,3], Masumi Tsuda[2,3], Tao Lin Sun[3,4], Kunpeng Cui[4], Riku Takahashi[1], Hui Jie Zhang[1], Tasuku Nakajima[3,4], Takayuki Nonoyama[3,4], Takayuki Kurokawa[3,4], Shinya Tanaka[2,3] and Jian Ping Gong[3,4*]*

[1]Graduate School of Life Science, Hokkaido University, Sapporo 001-0021, Japan, [2]Department of Cancer Pathology, Hokkaido University Faculty of Medicine, Sapporo 060-8638, Japan, [3]Global Institution for Collaborative Research and Education (GI-CoRE), Hokkaido University, Sapporo 001-0021, Japan, [4]Faculty of Advanced Life Science, Hokkaido University, Sapporo 001-0021, Japan.
Email: gong@sci.hokudai.ac.jp

Keywords: tough and thin hydrogel membrane, self-recovery, biocompatibility, biological membrane, anti-adhesive membrane

Abstract

Tough and self-recoverable hydrogel membranes with micrometer-scale thickness are promising for biomedical applications, which, however, rarely be realized due to the intrinsic brittleness of hydrogel. In this work, for the first time, by combing non-covalent DN statergy and spin-coating method, we successfully fabricated thin (thickness: 5-100 μm), yet tough (work of extension at fracture: ~10^7 J/m^3) and 100% self-recoverable hydrogel membranes with high water content (62-97 wt%) in large size (~100 cm^2). The excellent mechanical properties of these tough and thin gel membranes are comparable, or even superior to many biological membranes. The *in vitro* and *in vivo* tests show that these hydrogel membranes are biocompatible, and postoperative non-adhesive to neighboring organs. The excellent mechanical and biocompatible properties make these thin hydrogel membranes potentially suitable for use as biological or postoperative anti-adhesive membranes.

Keywords: thin hydrogel membrane; tough; self-recovery; biocompatibility; biological membrane; anti-adhesive membrane

1. Introduction

Owing to soft and wet nature, hydrogels are receiving ever increasing attention in various applications[1] including drug delivery[2–4], contact lenses[5], artificial organs[6], postoperative anti-adhesive membranes[7] and biological membranes[8,9]. Many of these potential applications require freestanding and even tough hydrogel membranes with micrometer-scale thickness. For example, as artificial substitutes for aponeuroses[10], skin[11], pericardium or septa, thin hydrogel membranes with high toughness and self-recovery are required. However, given the intrinsic brittleness of hydrogels, even for the free standing hydrogel membranes with micrometer-scale thickness, they usually need to be fabricated on supporting substrates[12] or composited with knitted fabrics and fibers[13], let alone the tough and self-recovery case. Fabrication of tough and self-recoverable hydrogel membranes of micrometer-scale thickness is a big challenge and urgently needed.

In the past decade, works on overcoming intrinsic brittleness of hydrogel has progressed tremendously, and a variety of tough hydrogels with different chemical structures has been developed[14]. Among them, the double network (DN) gels by introducing sacrificial bonds, invented in 2003, show both extremely high mechanical strength and toughness, even comparable to those of cartilages and rubbers[15]. The development of tough DN gels provide possibility for fabricating tough thin hydrogel membrane. However, it is not easy to extend the DN strategy from bulk gel to thin membrane directly. The challenge is, the requirement of a contrasting network structure formed by the two-step sequential polymerization sets a very high technical barrier for thin hydrogel membranes. Further, the first step for preparing DN gels is to synthesize a very brittle network, whose difficulty remarkably increases with decreasing thickness. Liang et al.[16] tried to synthesize DN hydrogels film by utilizing salt-controlled swelling and pre-reinforcing techniques. The thickness of obtained membrane is around 50 μm. Hu et al.[17] fabricated tough hydrogel membrane with thickness in several hundred μm by dispersing DN microgels into polyacrylamide matrix. However, above

methods are multi-step, operation sophisticating, and time-consuming. More importantly, those gel membranes exhibit permanent damage after large deformation, as the toughness arises from the fracture of irreversible covalent bond.

Here, in this work, for the first time, we successfully developed thin, yet tough, and self-recoverable hydrogel membranes having large surface area. Inspired by the recently developed self-recoverable physical DN hydrogels[18], we introduce the hydrogen bonds as sacrificial bonds to endow hydrogels membranes with self-recovery. This non-covalent strategy is further combined with spin-coating method to give a well-controlled thickness. The tough gel membranes developed along this line, referred to as "B-DN gel membranes", have substantially tunable thicknesses (5-100 μm), high stiffness (Young's moduli 0.1-110 MPa), high strength (fracture stress 1-8 MPa), high stretchability (fracture strain 100-1000%), high toughness (work of extension at fracture 10^5-10^7 J/m^3) and 100% fully self-recovery. These excellent mechanical properties are comparable, or even superior to many biological membranes. Moreover, these thin hydrogel membranes also possess high mechanical performance at physiological condition (in saline solution at 37 ^{o}C), and are biocompatible and anti-adhesive to the neighboring organs as demonstrated by the *in vitro* and *in vivo* tests. To the best of our knowledge, hydrogel membranes of micrometer-scale thickness that perform in this manner have never been previously achieved. These gel membranes show great potential as substitutes for biological or postoperative anti-adhesive membranes and this work also offers a new universal pathway to fabricate thin and tough hydrogels membranes.

2. Results and discussion

2.1 Structure uniformity

The thin first network membrane, referred to as the "B gel membrane", was prepared by spin coating of the triblock copolymer solution and following solvent exchange process. During spin coating process, inhomogeneous structure was easily formed due to the Marangoni-like instability, which appears once the solvent evaporated faster than diffusion

rate within the membranes[26-28]. To address this problem, the DMF was chosen as solvent, whose evaporation rate is very slow due to high vapor pressure. In addition, DMF vapor was introduced into spin-coater chamber to prevent solvent evaporation. To evaluate the solvent evaporation during spin coating process, the triblock copolymer concentrations (C_P) after spin coating were compared with that of initial states at various spin speeds. As shown in **Figure S1a**, the C_P has not obviously changed after spin coating at low spin speed, while above 3000 rpm, there is a slight increase of C_P due to little evaporation of solvent. Even so, the single first network gel (B gel) possesses uniform thickness from centers to edges (**Figure S1b**). To verify structure homogeneity, small-angle X-ray scattering (SAXS) experiments at different distance from center were performed (**Figure S1c~e**). The maximum scattering peak ($q1$) represents the distance between randomly-dispersed micelles in the gel[18]. As shown in **Figure S1f**, the peak positions ($q1$) of the membrane is independent of the distance from the center to the edge. Moreover, the azimuthal angle independence of the scattering profile indicates that no orientation structure formed in the gel membranes (insert of **Figure S1f**). The homogenous structure was also confirmed by the tensile stress-strain curves of B-DN gel membranes in the directions parallel with and vertical to the direction from the center to edge. As shown in **Figure S1g**, the tensile curves at the opposite directions almost overlap with each other, indicating the isotropic structure of the B-DN membranes.

2.2 Appearance and mechanical properties

Representative B-DN gel membranes are transparent and smooth **(Figures 1a, c**). Although the thickness only in micrometer-scale, those gel membranes show excellent mechanical property. For demonstration, a 36.2-um-thick membrane was impacted by a 120-g 30-mm-diameter ball, dropped from a height of 100 mm (inset **Figure 1a** and **Movie S1**). The sample withstood this impact without exhibiting any damage. In addition, these gel membranes were very flexible, robust, and could be easily folded into compact shapes without being damaged. **Figure 1b** illustrates the aspiration of a 16-cm^2-area, 36.2-μm-thick B-DN

gel membrane into a micropipette with a tip diameter of approximately 800 μm. The thin membrane could be easily sucked through the micropipette tip with a hole 3000 times smaller in area than that of the membrane. Furthermore, the B-DN gel membrane can be drawn back into the solution and recovered into its expanded-sheet form by gentle manipulation with a tweezer. The membrane can withstand at least 100 aspiration/drawing cycles without exhibiting any damage (**Movie S2**). The ability of the B-DN gel membrane to be "sucked" into such a tiny hole is another indication of its extremely high flexibility and toughness.

Figure 1d displays the stress-strain curve of a typical B-DN gel membrane and its counterparts, a B gel membrane and a PAAm gel membrane; the B-DN gel membrane, with a water content of ~75 wt%, has significantly enhanced mechanical properties compared to the PAAm gel membrane and the B gel membrane. Fracture stress (σ_b) and fracture strain (ε_b) of this B-DN gel membrane were 8.0 MPa at 940%, respectively. The extraordinary enhancement in mechanical strength possibly originates from the abundance of reversible sacrificial hydrogen bonds that are formed between the carboxyl groups of the midblock PMAAs and the amide groups of the second network poly(acrylamide)[18].

The B-DN gel membranes also exhibited 100% self-recovery. As shown by cyclic testing (**Figure 1e**), the B-DN gel membrane exhibits a large hysteresis for the first loading/unloading cycle, which dissipates a significant amount of energy. Subsequently, the loading/unloading curve can recover to that of virgin state over a waiting time of 20 min and 5 min for strain 50% and 30%, respectively (**Figure 1f**). To clarify the structure evolution during the cycle test, *in-situ* SAXS tests were also performed. The 2D SAXS images of the B-DN gel membrane measured in the virgin state, and that after-20 min recovery state are overlapped (**Figure S2**), which reveals that the structure completely recovers after sufficient waiting time. This recovery process is ascribed to competition between the elasticity of the primary network in the virginal state and the strength of the temporarily re-formed bonds. Due to elasticity of the primary network, the temporally re-formed hydrogen bonds are ruptured,

allowing the gel to recover to its equilibrium state. To the best of our knowledge, this is the first example of such a thin hydrogel membrane with such high toughness that is also 100% self-recoverable.

2.3 Thickness and mechanical tunability

The thickness and mechanical properties of the B-DN gel can be tuned by adjusting the concentration of the triblock copolymer, C_P, and the spin speed, *s*. **Figure 2a** reveals that these B-DN gel membranes with thicknesses ranging from 5 to 40 μm can be obtained from block polymer B_{273} at a constant spin speed 3000 rpm using C_P for the range 0.1-0.25 (wt/wt). The lower C_P limit (0.1) is close to the entanglement concentration of this block copolymer in DMF (data not shown). Below the entanglement concentration, the triblock copolymers form flower-micelle structures in which two endblocks are located in the same micelle rather than bridged between two micelles [22]. The upper limit (0.25) is related to the high viscosity of the solution. Above the concentration of 0.25, nonuniform gel membranes were observed during spin coating due to Marangoni-like instability[27,29]. The mechanical properties improve with increasing C_P due to an increase in the bridging fraction between neighboring micelles or the formation of more-effective hydrogen bonds between bridging chains and the second network at higher C_P values (**Figure S3a**). As clearly displayed in **Figure 2b**, for a constant C_P (e.g. 0.23), the thickness is easily tuned over the ~100 μm to ~10 μm range by increasing the spin speed from 500 to 5000 rpm. The tensile performance of the B-DN membranes appears to be independent of thickness at low spin speed; It should be noted that the tensile performance begins to decline as the spin speed exceeds 3000 rpm (**Figure S3b**), while these mechanical properties are still comparable or even superior to those of many biological membranes (**Tables S2 and S3**).

Given that the hydrogen bonds formed between the amides of the second network and the carboxyl groups of the first network are essential for endowing B-DN gel membranes with their excellent mechanical and self-recoverable properties, the molar ratio of the hydrogen-

bonding species was varied by changing the concentration (C_2) of the second monomer in the precursor solution. The tensile stress-strain curves of the B-DN gel membranes displayed in **Figure 2c** reveal that mechanical performance improves with increasing C_2, until a critical concentration point is reached (C_2 = 2 mol/L), where Young's modulus E and fracture stress σ_b reach their maximum values; this corresponds to a molar ratio of amides/carboxyl groups of 0.96 (**Figure 2e** and **Table S1**), which is close to the ideal 1:1 stoichiometric ratio. By continually increasing C_2, excessive numbers of hydrophilic amide groups create osmotic pressure that swells the B-DN gels and weakens the existing hydrogen bonds, resulting in decreased E and σ_b (**Figure S4**).

By assuming that hydrogen bonding is enhanced by hydrophobic interactions[23], the second monomer, AAm, was replaced by other amide-derived monomers bearing hydrophobic moieties, namely *N*,*N*-dimethylacrylamide (DMA) and *N*,*N*-diethylacrylamide (DEA). As shown in **Figure 2d**, the mechanical properties of the B-DN gel membranes strongly depend on the chemical structure of the second monomer. The B-DN gel membrane synthesized with AAm (C_2 = 0.5 M) does not exhibit a yielding point, whereas the B-DN gel membranes synthesized with the same concentration of DMA or DEA exhibit distinct yielding points. Furthermore, the B-DN gel membrane fabricated with DEA exhibits a large yielding stress (3.55 MPa) compared with that fabricated with DMA (2.38 MPa). These results are attributed to the hydrophobicities of the second monomers that follow the order: DEA > DMA > AAm. The more hydrophobic moieties the monomer has, the more stable the hydrogen bonds are, leading to enhanced yielding stress of the corresponding B-DN gel membrane.

This facile method for fabrication of B-DN gel membranes via the combination of spin-coating and the DN concept is general, which can be extended to a wide range of triblock copolymers. Based on this method, B-DN membranes from triblock copolymers with different midblock and total molecular-chain lengths were successfully fabricated (**Figure S5** and **Table S2**). The Young's modulus of these B-DN gel membranes was observed to increase

with decreasing midblock-chain length, whereas fracture strain is proportional to the length of the midblock chain. For example, Young's modulus increased from 0.15 to 1.97 MPa as the degree of polymerization of the midblock, n, decreased from 390 to 220; Young's modulus also decreased from 1.97 to 0.36 MPa when the total molecular length of the triblock copolymer was increased by a factor of 1.3.

In brief, these B-DN gel membranes, with 5-100-μm-thick and water contents of 62-97%, are tunable in Young's modulus over the 0.1-100 MPa range, while maintaining very high fracture stress (1-8.0 MPa), fracture strain (100%-1300%), and toughness (work of extension: ~10^5-10^7 J/m^3) (**Table S2**).

2.4 Stability in physiological condition

The excellent mechanical performance of these B-DN gel membranes indicates that they are promising as replacement for biological membranes, such as Glisson's capsules, pericardia, and gastrointestinal walls. For such biomaterial purposes, stability in physiological conditions (saline solution) are critically required for B-DN gel membranes. Typical tensile curves of the B-DN gel membranes in saline solution are shown in **Figure 3a**. The samples in saline solution show almost identical stress-strain curves to that obtained in pure water, indicating that the B-DN gel membranes are stable in saline solution possibly due to the stabilities of their hydrophobic micelles. The B-DN gel membranes also exhibit high mechanical performance in saline solution at human-body temperature (37 °C) (**Figure 3b and Table S4**). It should be mentioned that although the thin hydrogel membranes are easily dehydrated and become brittle in air, they are rapidly re-hydrated and recover to their original mechanical performances after being immersed in aqueous solution again (**Figure S6**).

2.5 Comparison of mechanical properties between B-DN membranes and various biological membranes

The mechanical properties of B-DN gel membranes were compared with those of various biological samples which contain 50-90% water at 10-1000 μm thickness. We found that the

mechanical properties of B-DN gel membranes overlap with, or are superior to those of the analyzed biological membranes (**Figure 4, Table S3**). While the fracture strain and toughness of B-DN gel membranes are superior to, the Young's modulus and fracture stress are comparable with, those of biological membranes. Additionally, mechanical performance of the B-DN membranes at 37 ^{o}C in saline solution (open circles) are also superior to those of biological membranes tested at 25 ^{o}C. These properties indicate the potential use of B-DN gel membranes as biological or postoperative membranes.

2.6 In vitro and in vivo biocompatibility

The biocompatibility of the B-DN gel membranes is demonstrated by both *in vitro* and *in vivo* tests. Prior to these tests, we have confirmed that the B-DN gel membranes withstand autoclavation process (120 °C, 7 min, and 101 kPa) and exhibit comparable tensile behavior before and after thermal sterilization (**Figure S7**).

For in vitro viability test, the 293T cells were cultured on three B-DN gel membranes, B-DN(AAm), B-DN(DMA), and B-DN(DEA), for 72 h and 120 h. Tissue culture polystyrene dish (TCPS) was used as a control. As shown in **Figure 5**, the trypan blue live/dead exclusion tests show that cell viabilities on these B-DN gel membranes are as high as on TCPS, being the common nontoxic cell cultivation material[24]. Throughout 120 h of cell cultivation, the viabilities of cells cultured on the B-DN gel membranes were maintained above 95%, confirming that B-DN gel membranes are not cytotoxic. While cell morphology varies when exposed to different types of B-DN gel membranes. When cultured on the B-DN(AAm) or B-DN(DMA) gel membranes, the cells packed into sphere shaped aggregates, suggesting a weak adhesion of the cells to these two gel membranes (**Figure 5a, e** and **b**, **f**); while the cells cultured on the B-DN(DEA) gel membranes show fibroblast-like morphology and form dome-shaped colonies (**Figure 5c, g**), similar to that on TCPS (**Figure 5d, h**), suggesting a relatively strong adhesion of the cells to this gel membranes. Such adhesion difference should be related to the difference in the hydrophobicity of the second polymer in B-DN gel

membranes. In comparison with AAm and DMA, the DEA is more hydrophobic and therefore more adhesive for cells**.** The results of increasing cell adhesiveness toward the increasing hydrophobic moieties in this study agree with those of other works[25,26].

Given that the DMA monomer itself is non-toxic and bio-inert, the B-DN(DMA) gel membrane was chosen for the *in vivo* biocompatibility test[27,28]. The B-DN(DMA) gel membranes were implanted underneath the rabbit skin and on surface of liver. The responses of the tissues were microscopically examined by pathologists at postoperative week 2. Representative histological images of the tissues for the subcutaneous experiment and liver experiment were shown in **Figure 6a, c**, respectively. Importantly, there was no inflammatory response and fibrosis found with the presence of gel membranes, as compared with the histological images of the control tissues without membrane implantation (**Figure 6b**, **d**), showing that the B-DN membranes did not induce any pathological reaction to the neighboring tissues. Furthermore, the B-DN membrane shows no microscopical adhesion to the surrounding organs, indicating the potential use of B-DN membranes as anti-adhesive sheets to reduce postoperative tissue adhesion formation which is one of the major problems after various surgical procedures. The mechanical robustness and biocompatibility of these B-DN gel membranes provide the opportunities to construct artificial tissue membranes and surgical anti-adhesive membranes using synthetic materials.

3. Conclusion

In summary, we successfully synthesized freestanding tough B-DN gel membranes with micrometer-scale thicknesses based on the DN concept. At such low thickness, the B-DN gel membranes exhibit super-high strength, toughness, and full self-recoverability. They have comparable Young's modulus and much higher fracture toughness compared with biological membranes. Moreover, the thin B-DN gel membranes were highly tolerant to biological environments, biocompatible, and not adherent to biological tissue in vivo. These results

demonstrate the sheer variety and potential use of such soft and wet hydrogel materials as biological and postoperative anti-adhesive membranes.

4. Experimental Section

Materials: The amphiphilic triblock copolymers, poly(butyl methacrylate)-*b*-poly(methacrylic acid)-*b*-poly(butyl methacrylate) (PBMA-*b*-PMAA-*b*-PBMA) with various degrees of polymerization, were synthesized by the Otsuka Chemical Co., Ltd., Japan (**Table 1**). The second monomers acrylamide (AAm), *N*,*N*-dimethylacrylamide (DMA) and *N*,*N*-diethylacrylamide (DEA), the initiator 2-oxoglutaric acid, and the solvent dimethylformamide (DMF) were purchased from Wako Pure Chemical Industries, Ltd. (Japan). Alexa Fluor^{TM} 594 phalloidin and DAPI (4',6-diamidino-2-phenylindolewere) and culturing media were purchased from Invitrogen Japan KK (Tokyo, Japan).

Hydrogel membrane preparation: The schematic illustration of the preparation process is shown in **Scheme 1**. The triblock copolymers were dissolved in dimethylformamide at different concentrations, C_P, of 0.1-0.25 (wt/wt). The membranes were fabricated by spinning a 5-mL triblock copolymer/DMF solution for 30 s at prescribed spin speed in a sample cell with controlled solvent vapor pressure. The thin membrane was then immersed in water to form the first network, B gel membrane, via hydrophobic association of the PBMA blocks. After reaching equilibrium, the B gel membrane was immersed in an aqueous solution containing prescribed concentrations of the second monomer and 2-oxoglutaric acid (0.05 mol% relative to the second monomer) as UV-initiator for several minutes, followed by irradiation with 365 nm UV light for 8 h. Following polymerization, the as-prepared B-DN gel membrane was immersed in purified water for 10 min to reach equilibrium. The sample codes of B-DN gel membranes were shown in **Table 2**. For comparison, the pure PAAm gel membrane was prepared from a precursor solution containing 2 mol/L AAm, 0.05 mol%

MBAA, and 0.05 mol% 2-oxoglutaric acid in a reaction cell and polymerized at condition mentioned above.

Water content measurement: The water contents of B-DN gel membranes were measured using a moisture balance MOC-120H (Shimadzu Co. Japan). During test, water was gradually evaporated from the hydrogel at an elevated temperature from 25 °C to 120 °C. The water content was defined as $c_w = (1\text{-}m_1/m_0) \times 100\%$, where the m_0 and m_1 are the weight of the sample in wet and dry states, respectively.

Thickness measurement: The membrane thicknesses were obtained in triplicates via a 3D violet laser scanning microscope (VK-8700, KEYENCE Co., Ltd.) by step height measurement. The thickness of thin hydrogel membrane is defined by the orthogonal distance between two parallel planes representing the upper surface (red profile) of the membrane and a layer of the base material (substrate) contacting the lower surface (light gold profile), respectively (**Figure 1c**).

Swelling ratio: The thickness swelling ratio $Q = t/t_0$ is defined as the ratio of the sample thickness, t of B-DN gel membranes to that of B gel membranes t_0 at swelling equilibrium.

Tensile and cyclic test. The tensile stress-strain measurements were performed using a tensile-compressive tester (Tensilon RTC-1310A, Orientec Co.) at a deformation velocity of 10 mm/min at 25 ^oC in water bath and 37 ^oC in saline solution to prevent evaporation. The work of extension at fracture W_b (J/m^3), a parameter that characterizes the work required to fracture the sample per unit volume, was calculated from the area below the tensile stress-strain curve until fracture. The fracture stress σ_b and the fracture strain ε_b were defined as nominal stress and strain at fracture point, respectively. The Young's modulus E was defined as value of initial slope of the stress-strain curve. The cyclic tensile tests were carried out in a humidity controlled environment at velocity of 10 mm/min with maximum strain of 30% and 50%, respectively. Tensile and cyclic test were carried out on dumbbell-shaped samples with

the standard JIS-K6251-7 size (12 mm (gauge length) × 2 mm (width) × 5~100 μm (thickness)).

Small angel X-ray scattering (SAXS): The static SAXS measurements were performed at BL40B2 beamline at the Synchrotron X-ray Facility in SPring-8. The wave length of X-ray was 1.0 Å and the sample-to-detector distance was set to be 2310 mm. The *in-situ* SAXS measurements were performed at BL19U2 beamline at the National Center for Protein Sciences Shanghai. The wavelength of X-ray was 1.033 Å and the sample-to-detector distance was set to be 6225.6 mm. During *in-situ* test, the samples were fixed on a uniaxial stretching machine. The data acquisition time was 20 s per frame for the two-dimensional (2D) SAXS images. All scattering images were analyzed with Fit2D software from European Synchrotron Radiation Facility by taking off the detector spatial distortion, X-ray beam fluctuation and background scattering.

To investigate the physical properties similarity of B-DN hydrogel membranes and biological membranes, water content, thickness and tensile stress-strain measurements for Glisson's capsule, pericardium, gastrointestinal wall, heart wall, intestine, aorta vessel, ovary capsular and skin, were performed at condition mentioned above.

In vitro viability and morphology: Prior to cell cultivation, the B-DN hydrogels were sterilized in PBS and equilibrated for 1 day in Dulbecco's modified Eagle's medium (DMEM) supplemented with 1% Penicillin Streptomycin, 2 mM l-glutamine, and 10% fetal bovine serum. The human embryonic kidney cells with a concentration of $2x10^4$ cells/mL were seeded onto B-DN gel membranes and polystyrene control. Live/Dead cell counts were obtained by trypan blue exclusion test (n = 3) after incubating (5% CO_2 humidified atmosphere, 37 °C) for 72 h and 120 h.

Cell morphology was observed after 120 h cultivation through bright field (Olympus IX 73) and fluorescence microscopy (Keyence BZ-9000). For the immunofluorescence staining with DAPI (cell core) and phalloidin (actin filament), cells were fixed for 15 min in 3%

paraformaldehyde, permeabilized in 0.1% Triton X-100 for 4 min, stained with Alexa Fluor 594 conjugated phalloidin for 30 min followed by 1 μg/mL DAPI in 1% BSA supplemented PBS for 15 min at room temperature (2-3 PBS washing steps after each procedure).

In vivo compatibility: Animal experiments were carried out in the Institute of Animal Experimentation, Hokkaido University Faculty of Medicine under the Rules and Regulation of the Institutional Animal Care and Use Committee of National University Corporation Hokkaido University.

A total of 9 female Japanese white rabbits (3.0-3.5 kg) were used in this study. The B-DN gel membranes were implanted into subcutaneous region (n = 4) or onto liver surface (n = 5). Prior to the implantation, B-DN gel membranes were washed three times with autoclaved Millipore-filtrated water, immersed in saline solution for 1 week with daily buffer substitution, and autoclaved. The surgery was performed under isoflurane anesthesia. For subcutaneous implantation, 5 cm incision was made with a scalpel on the rabbit ventral skin, and the B-DN membranes (5.0 × 4.0 cm) were subcutaneously implanted onto muscle *in vivo*. For the transplantation on liver surface, the B-DN membranes (4.0 × 4.0 cm) were implanted onto the liver surface. The rabbits were euthanized at 2 postoperative weeks, and the subcutaneous tissue and the liver were resected with the B-DN membranes and formalin-fixation was performed for 3 days. For histological examination, the tissues were stained with hematoxylin and eosin (H&E) and evaluated by pathologists microscopically.

Supporting Information

Supporting Information is available from the Wiley Online Library or from the author.

Acknowledgements

We thank Mr. Osamu Ito and Mr. Hiroyuki Ishitobi (Otsuka Chemical Co., Ltd.) for their kind donation of the triblock copolymers. The static SAXS experiments were performed at the BL40B2 of SPring-8 with the approval of the Japan Synchrotron Radiation Institute (JASRI) (Proposal number: 2016A1254). The *in-situ* SAXS experiments were performed at

NCPSS BL19U2 beamline at National Center for Protein Sciences Shanghai. We thank the staff (Na Li, Guangfeng Liu and Hongjin Wu) for assistance during data collection. We also thank Prof. Liangbin Li (University of Science and Technology of China) for providing the special-made tensile tester for *in-situ* SAXS experiments. This research was supported by JSPS KAKENHI Grant Numbers JP24225006, JP17H06144, and JP17H04891. This research was also supported by the ImPACT Program of Council for Science, Technology and Innovation (Cabinet Office, Government of Japan). Y. N. Y. thanks the MEXT, Japan for a scholarship during her PhD studies.

Received: ((will be filled in by the editorial staff))
Revised: ((will be filled in by the editorial staff))
Published online: ((will be filled in by the editorial staff))

References

[1] A. L. Rutz, R. N. Shah, In *Polymeric Hydrogels as Smart Biomaterials*; Springer, 2016; pp. 73–104.

[2] Y. Jiang, J. Chen, C. Deng, E. J. Suuronen, Z. Zhong, *Biomaterials* **2014**, *35*, 4969.

[3] J. Wu, A. Chen, M. Qin, R. Huang, G. Zhang, B. Xue, J. Wei, Y. Li, Y. Cao, W. Wang, *Nanoscale* **2015**, *7*, 1655.

[4] X. Wang, T. Yucel, Q. Lu, X. Hu, D. L. Kaplan, *Biomaterials* **2010**, *31*, 1025.

[5] P. Paradiso, A. P. Serro, B. Saramago, R. Colaço, A. Chauhan, *J. Pharm. Sci.* **2016**, *105*, 1164.

[6] C. Mandrycky, Z. Wang, K. Kim, D.-H. Kim, *Biotechnol. Adv.* **2016**, *34*, 422.

[7] H. Torii, T. Takagi, M. Urabe, H. Tsujimoto, Y. Ozamoto, H. Miyamoto, Y. Ikada, A. Hagiwara, *J. Obstet. Gynaecol. Res.* **2017**, *43*, 1317.

[8] K. Y. Lee, D. J. Mooney, *Chem. Rev.* **2001**, *101*, 1869.

[9] M. A. Daniele, A. A. Adams, J. Naciri, S. H. North, F. S. Ligler, *Biomaterials* **2014**, *35*, 1845.

[10] C. N. Maganaris, M. V Narici, In *Tendon Injuries*; Springer, 2005; pp. 14–21.

[11] P. P. Purslow, *J. Mater. Sci.* **1983**, *18*, 3591.

[12] I. Tokarev, S. Minko, *Soft Matter* **2009**, *5*, 511.

[13] C. D. Young, J. R. Wu, T. L. Tsou, *Biomaterials* **1998**, *19*, 1745.

[14] Y. S. Zhang, A. Khademhosseini, *Science (80-.).* **2017**, *356*, 3627.

[15] J. P. Gong, Y. Katsuyama, T. Kurokawa, Y. Osada, *Adv. Mater.* **2003**, *15*, 1155.

[16] S. Liang, Q. M. Yu, H. Yin, Z. L. Wu, T. Kurokawa, J. P. Gong, *Chem. Commun.* **2009**, *48*, 7518.

[17] J. Hu, K. Hiwatashi, T. Kurokawa, S. M. Liang, Z. L. Wu, J. P. Gong, *Macromolecules* **2011**, *44*, 7775.

[18] H. J. Zhang, T. L. Sun, A. K. Zhang, Y. Ikura, T. Nakajima, T. Nonoyama, T. Kurokawa, O. Ito, H. Ishitobi, J. P. Gong, *Adv. Mater.* **2016**, *28*, 4884.

[19] M. Malmsten, B. Lindman, *Macromolecules* **1992**, *25*, 5440.

[20] D. E. Bornside, C. W. Macosko, L. E. Scriven, *J. Appl. Phys.* **1989**, *66*, 5185.

[21] P. Mokarian-Tabari, M. Geoghegan, J. R. Howse, S. Y. Heriot, R. L. Thompson, R. A. L. Jones, *Eur. Phys. J. E* **2010**, *33*, 283.

[22] T. L. Chantawansri, T. W. Sirk, Y. R. Sliozberg, *J. Chem. Phys.* **2013**, *138*, 24908.

[23] X. Hu, M. Vatankhah-Varnoosfaderani, J. Zhou, Q. Li, S. S. Sheiko, *Adv. Mater.* **2015**, *27*, 6899.

[24] W. Strober, *Curr. Protoc. Immunol.* **2015**, A3.B.1.

[25] J. H. Lee, H. B. Lee, *J. Biomater. Sci. Polym. Ed.* **1993**, *4*, 467.

[26] Y. Arima, H. Iwata, *Biomaterials* **2007**, *28*, 3074.

[27] K. Arakaki, N. Kitamura, H. Fujiki, T. Kurokawa, M. Iwamoto, M. Ueno, F. Kanaya, Y. Osada, J. P. Gong, K. Yasuda, *J. Biomed. Mater. Res. Part A* **2010**, *93*, 1160.

[28] Y. Tanabe, K. Yasuda, C. Azuma, H. Taniguro, S. Onodera, A. Suzuki, Y. M. Chen, J. P. Gong, Y. Osada, *J. Mater. Sci. Mater. Med.* **2008**, *19*, 1379.

Table 1. Description of triblock copolymers.

Code	Triblock copolymer [a] $A_mB_nA_p$	[b] f_B	[c] Mw (kg/mol)	[d] M_w/M_n
B_{390}	$A_{141}B_{390}A_{141}$	0.58	73.66	1.43
B_{297}	$A_{145}B_{297}A_{117}$	0.52	62.86	1.38
B_{220}	$A_{157}B_{220}A_{146}$	0.42	62.00	1.25
$1.3B_{220}$	$A_{247}B_{334}A_{215}$	0.42	74.22	1.46

[a] The subscripts of m, n and p represent the degree of polymerization of the endblock, midblock and endblock respectively. A and B represent poly(butyl methacrylate) (PBMA) and poly(methacrylic acid) (PMAA), respectively. [b] Molar fraction of midblock PMAA. [c, d] Weight-average molecular weight and molecular weight distribution of the triblock copolymer, respectively.

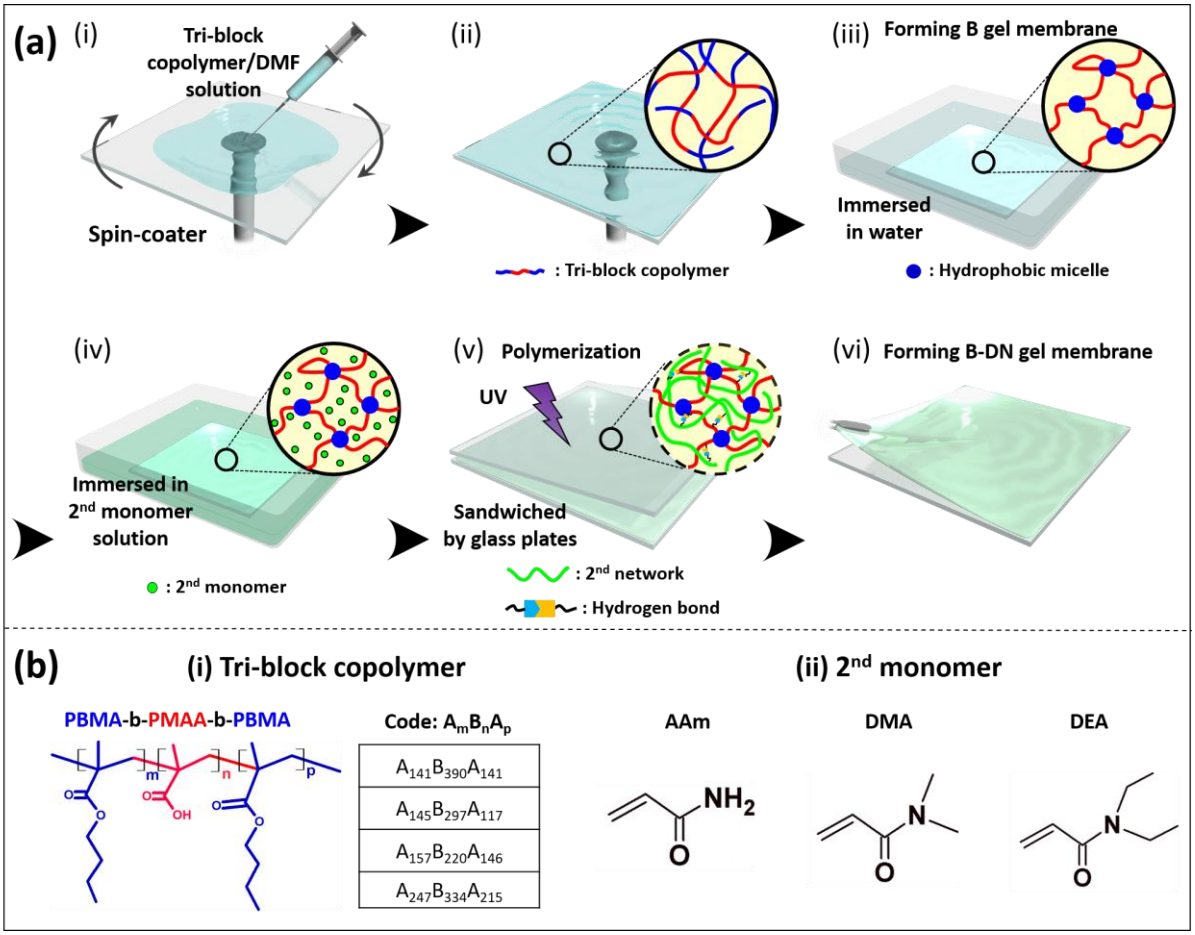

Scheme 1. Schematic diagram depicting the preparation of a thin B-DN gel membrane. (a) The spin-coated thin tri-block copolymer membrane was fabricated by depositing ~5 mL triblock copolymer solution onto a spin plate, followed by rapid acceleration of spin speed. After spin-coating, the thin membrane was immersed in water to initiate the hydrophobic chain self-assembly that forms the weak B gel membrane as the first network. After reaching equilibrium, the B gel membrane was immersed in an aqueous solution of the second monomer/UV-initiator and allowed to soak for several minutes. Finally, the second monomers were polymerized for 8 h to form polymers that can physically associate with the first network. (b) Chemical structures of the triblock copolymers that form the physical B-gel as the first network, and the second monomers that form linear chains as the second network.

Table 2. Sample codes and formulations of the B-DN gel membranes.

Sample code [a] B_n (C_P-s/*m*-C_2)	1st network		2nd network	
	Triblock polymer concentration, C_p (wt/wt)	Spin speed, *s* (rpm)	2nd monomer, *m*	Concentration, C_2 (mol/L)
B_{273} (C_P-3000/AAm-2)	0.1~0.25	300	AAm	2
B_{273} (0.23-s/AAm-2)	0.23	500~5000	AAm	2
B_{273} (0.23-3000/m-2)	0.23	3000	AAm, DMA, DEA	0.5
B_{273} (0.23-3000/AAm-C_2)	0.23	3000	AAm	0.2~7

a) *n* is the degree of polymerization of the midblock in the triblock copolymer, C_P is the weight fraction of the triblock copolymer in the precursor DMF solution used for the preparation of the spin-coated membranes, *s* is the spin speed (rpm), *m* is the 2nd monomer type, and C_2 is the concentration of the second monomer (mol/L) in the aqueous precursor solution used for the polymerization of the second monomers. The second monomer was polymerized using an initiator concentration of 0.05 mol% (relative to the second monomer) in the absence of a chemical crosslinker.

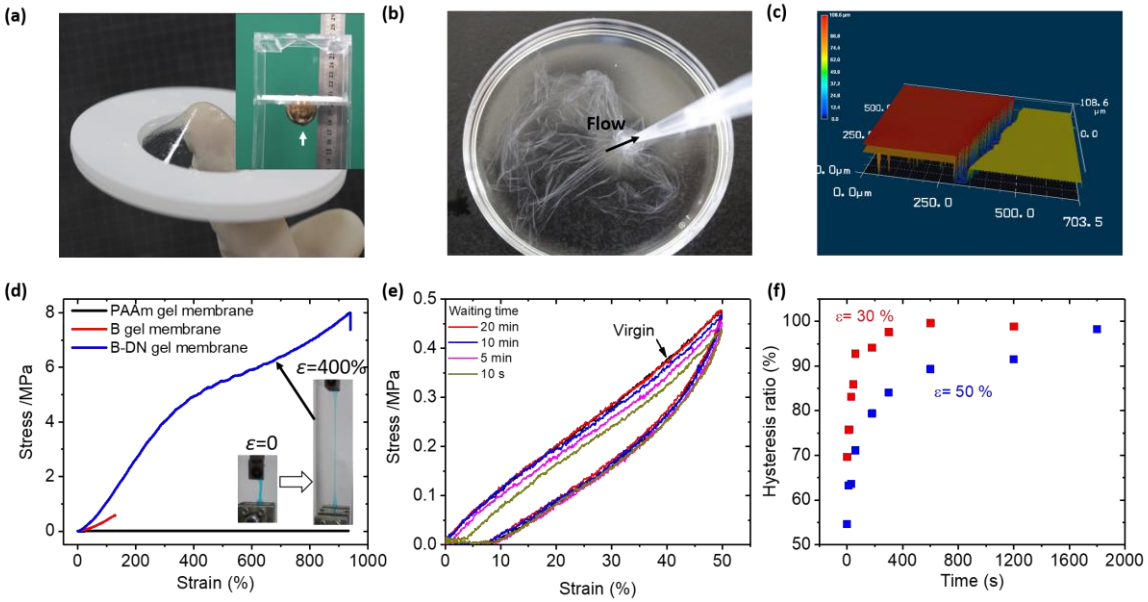

Figure 1. (a) Optical images of a 36.2-μm-thick B-DN gel membrane sustaining the impact of a 120-g ball (white arrow) falling from a height of 100 mm (inset image). (b) Optical image showing aspiration of the B-DN gel membrane (36.2-μm-thickness, 16-cm^2-area) into a micropipette (tip diameter: 800 μm). (c) 3D laser microscope image of the surfaces the B-DN membrane (red profile) and the glass substrate (light gold profile). Sample code: B_{273} (0.23-3000/AAm-2). (d) Tensile stress-strain curves for the B-DN gel membrane and its counterparts. A PAAm gel membrane (thickness: 523 μm); a B gel membrane (thickness: 34.2 μm); a B-DN gel membrane: B_{273} (0.23-3000/AAm-2), thickness: 36.2 μm. The insets depict the B-DN gel membrane in its virgin state (ε = 0) and the stretched state (ε = 400%). The gel membrane has been dyed for clarity. (e) Waiting time dependence of the cyclic tensile test results (strain:50%), and (f) Hysteresis ratio (ratio of the area of a subsequent hysteresis loop to that of the virgin) as functions of waiting time (Strain: 30% and 50%). Sample code: B_{273} (0.23-500/AAm-2), thickness: 113 μm.

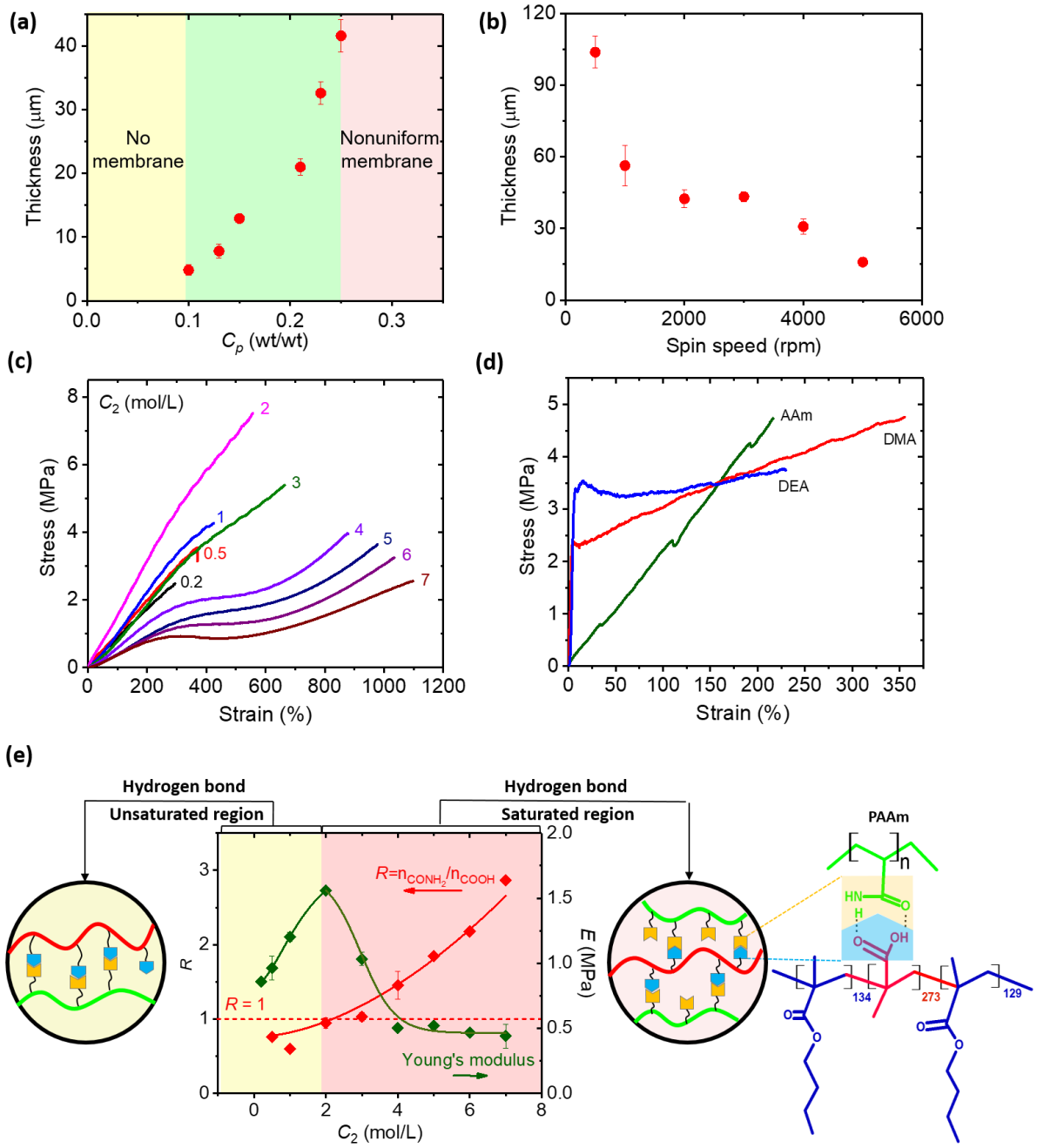

Figure 2. (a) Thickness of the B-DN gel membrane as a function of the triblock copolymer concentration (C_P) of precursor solution. Sample code: B_{273} (C_P-3000/AAm-2). (b) Thickness of the B-DN gel membrane as a function of spin speed, *s*. Sample code: B_{273} (0.23-*s*/AAm-2). (c) Tensile behavior of B-DN gel membranes prepared using different concentrations (C_2) of the second AAm monomer. Sample code: B_{273} (0.23-3000/AAm-C_2). (d) Tensile behavior of the B-DN gel membranes with different second networks. Sample code: B_{273} (0.23-3000/*m*-0.5). (e) Molar ratio *R* of the amides in the second polymer to the carboxyl groups of the PMAA units in the B-DN gel membrane as determined by element analysis. The red horizontal dotted line denotes a 1:1 molar ratio of the amide to carboxyl groups. Sample code: B_{273} (0.23-3000/AAm-C_2).

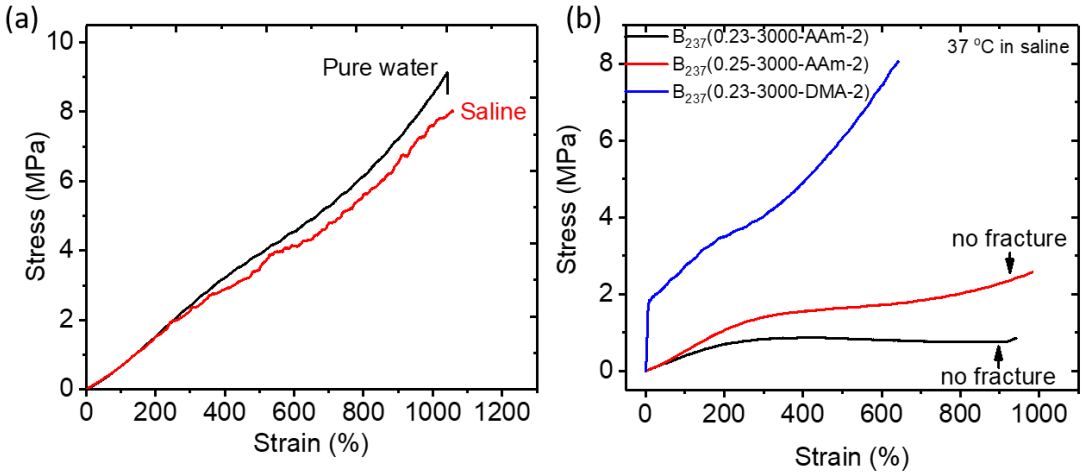

Figure 3. (a) Tensile behavior of the B-DN gel membrane at room temperature in pure water and saline solution. Sample code: B_{273} (0.23-3000/AAm-2), thickness: 30.4 ± 0.6 μm. (b) Tensile behavior of the B-DN gel membrane at 37 °C in saline solution, Sample codes were shown in the figure.

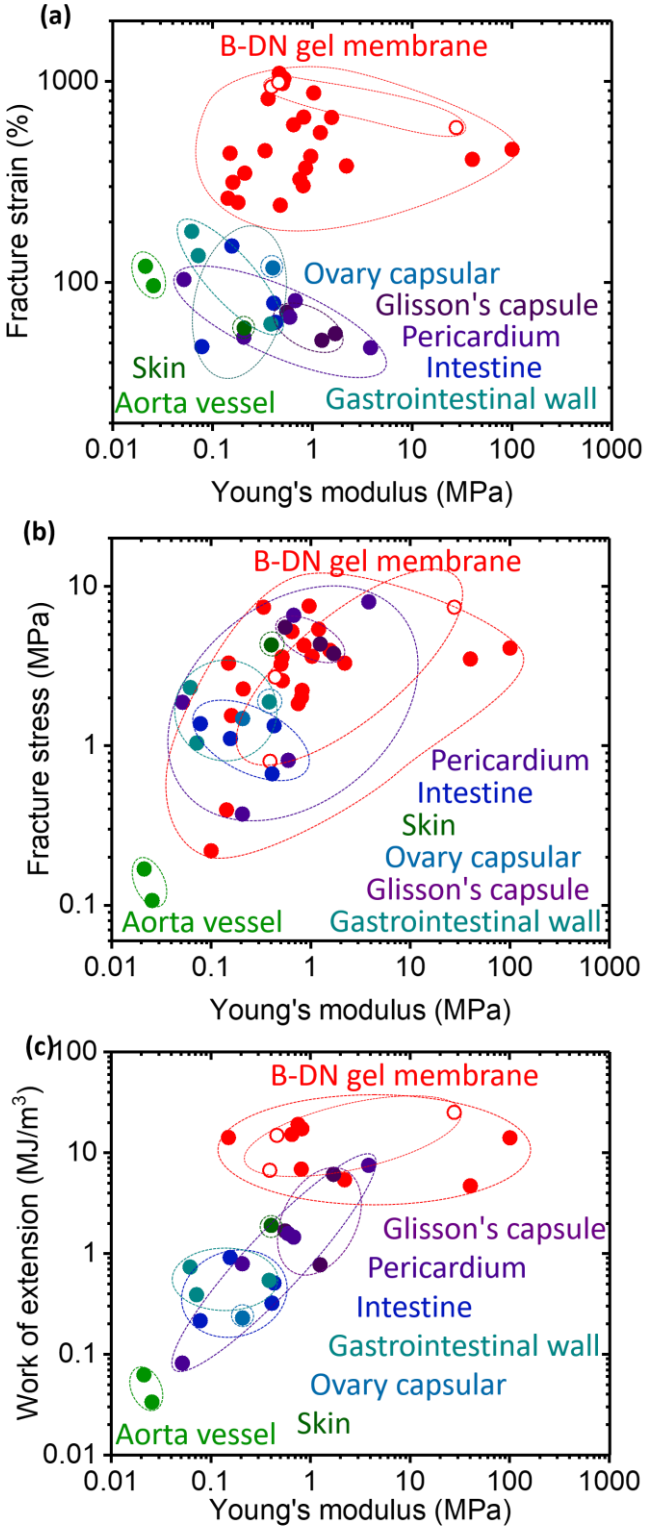

Figure 4. The mechanical properties of the B-DN gel membranes developed in this work and various biological membranes. (a) Fracture strain vs. Young's modulus; (b) fracture stress vs. Young's modulus; (c) Work of extension vs. Young's modulus. Numerical data are listed in Tables S2 and S3 for the B-DN gel membranes and the biological membranes, respectively. The closed red circles were results measured at 25°C and the open red circles were measured at 37 °C for B-DN gel membranes.

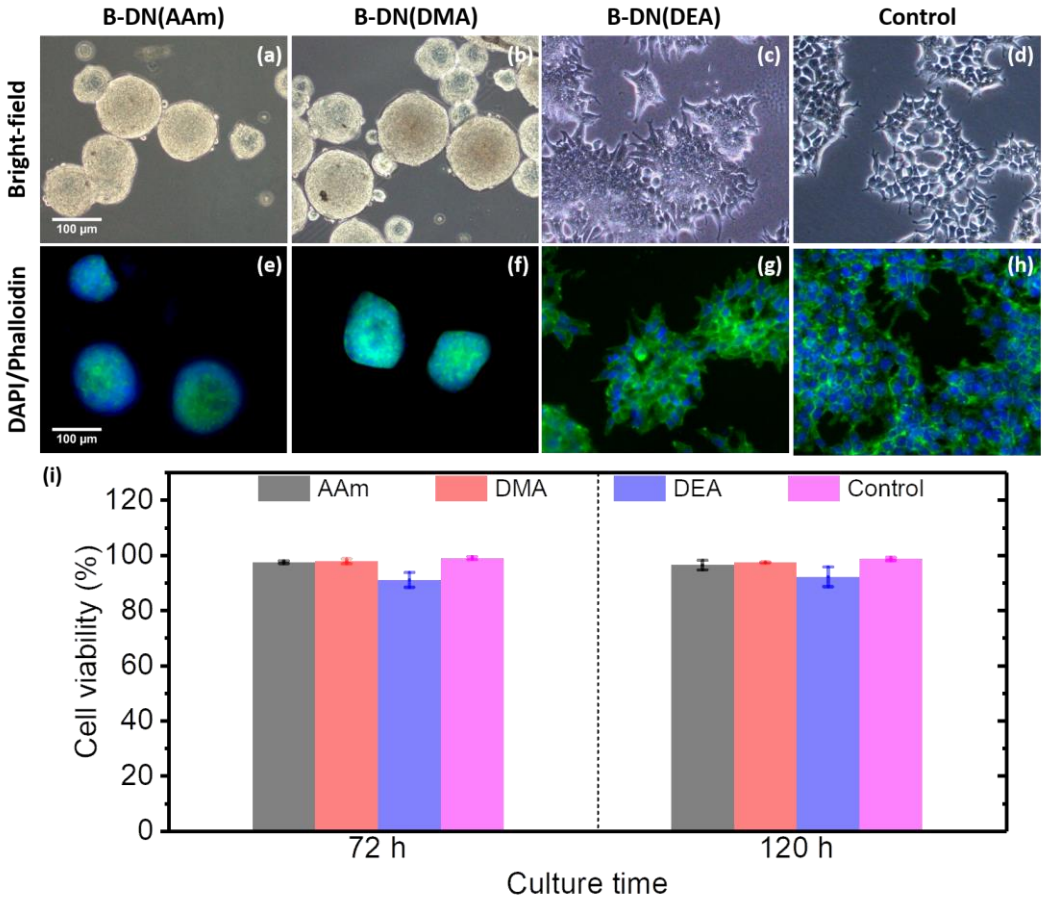

Figure 5. Photographs taken by bright field microscopy of 293T cell cultured on a B-DN gel membrane prepared by second monomers (a) AAm, (b) DMA and (c) DEA for 120 h, respectively. The tissue culture polystyrene (TCPS) was used as a control (d). The corresponding immunofluorescence images of (a-d) were shown in (e-h) at 20x magnification. (i) Viability of 293T cells cultured on the TCPS control and a B-DN gel membrane for 72 h and 120 h for various B-DN gel membranes. Sample code: B_{273} (0.23-2000/AAm-2), thickness: 44.1 ± 8.1 μm, B_{273} (0.23-2000/DMA-2), thickness: 47.5 ± 5.1 μm, B_{273} (0.23-2000/DEA-2), thickness: 32.7 ± 2.3 μm.

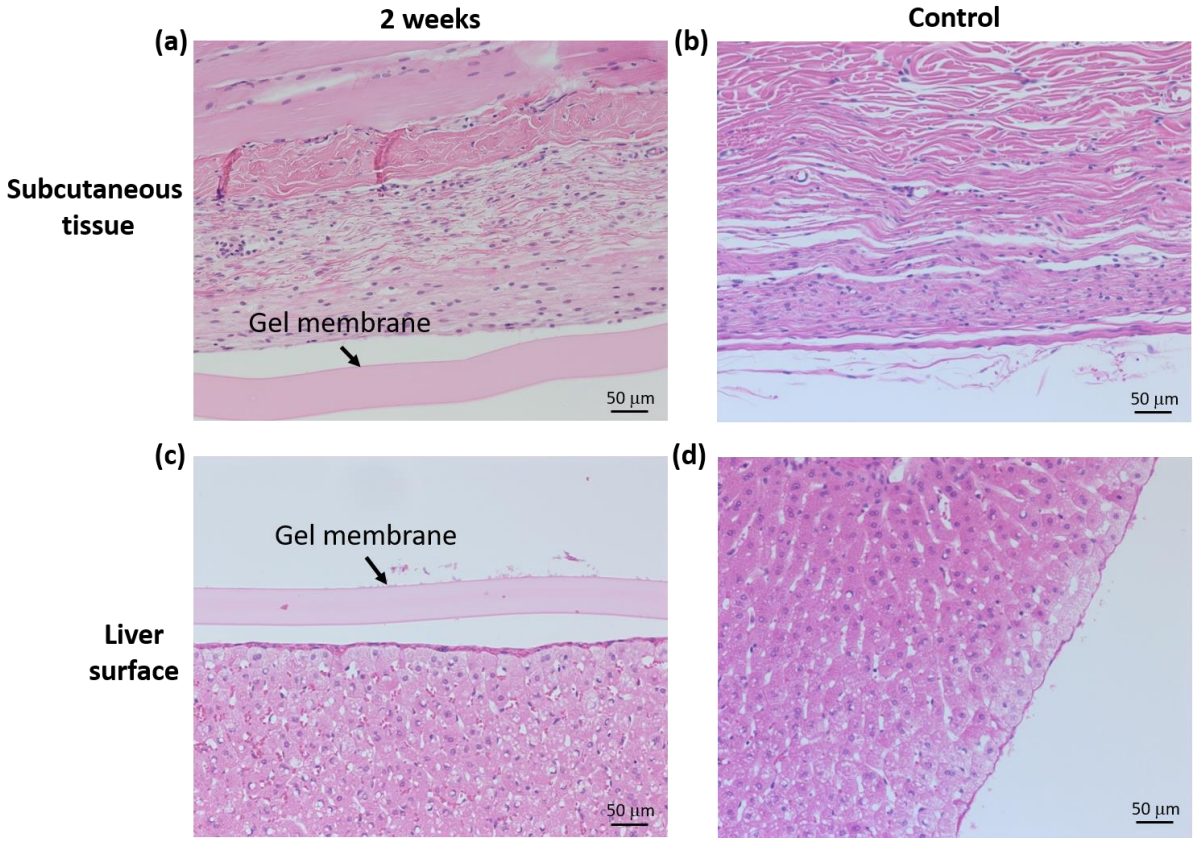

Figure 6. Microscopic observations of hematoxylin- and eosin-stained sections of subcutaneous tissue (a) and liver surface (c) implanted with B-DN gel membranes at postoperative weeks 2. (b) and (d) are the corresponding normal tissue as control without B-DN gel membranes implantation. Black arrows indicate the B-DN gel membranes. Sample code: B273(0.23-2000/DMA-2), thickness: 47.5 ± 5.1 μm.